Eye Pattern Evaluation in High-Speed Digital Systems Analysis by Using MTL Modeling

Giulio Antonini, *Member, IEEE*, James L. Drewniak, *Senior Member, IEEE*, Antonio Orlandi, *Senior Member, IEEE*, and Vittorio Ricchiuti, *Senior Member, IEEE*

***Abstract*—A method for simulating the eye pattern of high-speed digital signals propagated on printed circuit boards using multiconductor transmission-line modeling is proposed in this paper. The approach takes into account the frequency-dependent properties of the dielectric materials of the board and of the conductors. The validation is performed by comparing the modeling with measurements taken from the literature, and directly performed on test boards specially design for this study.**

***Index Terms*—Dielectric constant, dissipation factor, frequency-dependent dielectric, signal integrity.**

I. Introduction

MODERN broad-band telecommunication systems are characterized by optical interfaces with high data transfer rates. At present, optical signals at 10 Gb/s are relatively commonplace in transmission equipment. These optical signals are converted into electrical digital signals at high bit rates, which are directly managed by the high-speed digital devices. The present generation of high-speed digital chips for telecommunication use high-speed serial links (HSSLs) up to 3.125 Gb/s to transport data on printed circuit boards (PCBs). HSSLs have become a necessity in the modern digital boards because they allow one to exchange a large amount of data between application-specific integrated circuits (ASICs), reducing the pin count on the semiconductor device packages so as to obtain cost savings. The next step in the semiconductor industry is to realize chips operating with clock rates up to 10 GHz by 2010 [1]. This innovation in the semiconductor world will produce a new challenge in the PCB world, in particular, designing board interconnections with very high performances in the frequency range up to 20 GHz. Differential signaling will be employed to accomplish this due to its lower susceptibility to common mode noise than single-ended signaling, which maximizes noise margins in the link.

As the bandwidth of the HSSLs goes beyond 1 GHz, signal integrity (SI) problems become a primary concern for PCB designers [2], [3]. One of the most common SI problems is the attenuation of high-bandwidth digital signals over the PCB trace lengths. At high bit rates, low-cost FR-4 materials, a mix of glass fiber and epoxy resin, currently used in the telecommunication and computer industry to fabricate PCBs [4], is characterized by high dielectric loss factors, so that the frequency-dependent losses over the typical PCB trace lengths are too large. To overcome this problem, which causes amplitude fluctuations and jitter on the signals along the traces, alternative lower dielectric loss PCB materials are used [5]–[7].

Usually, SI problems along a trace, due to their nature, are studied in the time domain, using, for example, eye pattern measurements. The eye pattern allows the quality of the signal at the end of a trace to be characterized. The larger the eye is opened, the better the signal quality is at the termination end of the line. Amplitude distortion of the signal along the trace, due to discontinuities or losses, reduces the eye opening and the noise margin, so that the receiver at the end of the line has difficulties in correctly detecting the signal. The eye pattern width gives information about the time interval where the data can be sampled at the receiving end without problems due to intersymbol interference (ISI). Such a width can be reduced by the jitter due to the dispersion along the interconnection.

Although time-domain measurements can be interpreted easily and are directly relevant to the function of the digital device, frequency measurements are being increasingly used to characterize signal propagation on PCBs and study SI problems [7]–[9]. This characterization is more accurate and reliable than that in the time domain due to the higher dynamic range and more robust calibration procedure of a network analyzer, as compared to a time-domain reflectometer (TDR). Moreover, time-domain magnitudes can be obtained from frequency-domain measurements by using inverse fast Fourier transforms (IFFTs). The eye pattern, e.g., at the end of a trace, is obtained by convolving the IFFT of the scattering parameter S_{21} along the trace, measured in the frequency domain, with a repetitive bit pattern. When the impact on SI of the properties of the dielectric material [relative permittivity $\varepsilon_r(\omega)$ and dissipation factor $\tan\delta(\omega)$] must be assessed, the prediction of the eye pattern is needed in the design cycle prior to building physical boards. In this case, the approach cited above, which is based on the measurement of S_{21}, is unsatisfactory.

The Telegrapher's equations can be solved for the source and load voltages using multiconductor transmission line (MTL) modeling [10], assuming the model holds for microstrip and stripline structures. The fundamental assumption for all transmission line formulation and analysis is that the field structure surrounding the conductors obeys a TEM structure; the transmission lines considered for this work have cross-sectional di-

Manuscript received July 16, 2001.

G. Antonini and A. Orlandi are with the Department of Electrical Engineering, University of L'Aquila, I-67040 L'Aquila, Italy (e-mail: orlandi@elettrica.ing.uniroma1.it).

J. L. Drewniak is with the Electromagnetic Compatibility Laboratory, Electrical and Computer Engineering Department, University of Missouri-Rolla, Rolla, MO 65409-0040 USA.

V. Ricchiuti is with CNX S.p.A.—A Siemens Company, I-67100 L'Aquila, Italy.

Publisher Item Identifier 10.1109/TMTT.2002.800443.

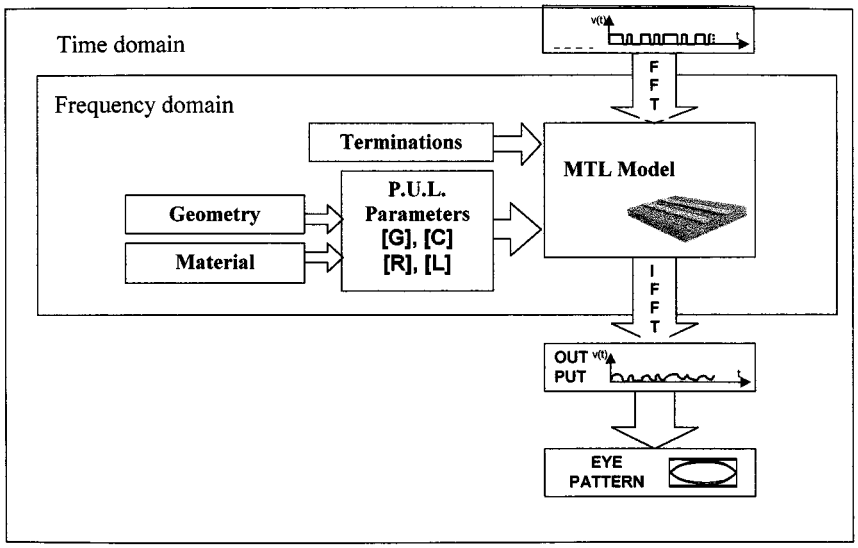

Fig. 1. Schematic flow chart for the TFTD method.

mensions smaller than the minimum wavelength associated with the spectra of the propagating signal and, hence, can be assumed to be TEM structures. Then, from the load voltage, it is possible to extract the eye pattern.

The objective of this paper is the development of a procedure to predict the eye pattern due to a digital bit pattern propagating on microstrip and stripline structures with single-ended and differential terminations without relying on experimental data. The frequency-dependent properties of the dielectric are included in the formulation. The proposed procedure is comprised of three primary steps: 1) extraction of the per unit length (p.u.l.) parameters; 2) solution of the MTL equations; and 3) eye pattern formation. The procedure is developed in frequency domain by applying a *time-to-frequency-to-time domain* (TFTD) approach for the solution of the MTL equations. This approach is described in Section II. Section III illustrates eye pattern simulations and measurements in order to validate the approach and to formulate guidelines for the digital design. Conclusions are drawn in Section IV.

II. TFTD Approach

The MTL equations are first solved in frequency domain in the TFTD approach. The frequency spectrum of the source voltage is obtained by means of a fast Fourier transform (FFT) of a pseudorandom bit sequence (PRBS) generated in the time domain. The time waveforms of the voltages and currents along the line and across the loads are obtained by means of an IFFT, as schematically depicted in the flow chart of Fig. 1. Then, consider an $n+1$ conductor transmission line of length L, as shown in Fig. 2(a). Due to the multiconductor nature of the line, the voltage, current, and impedance variables are vectors or matrices, which will be indicated by bold letters. $\hat{\mathbf{V}}_\mathbf{S}$ and $\mathbf{Z}_\mathbf{S}$ are the phasor voltage and internal impedance of the voltage source, respectively, $\mathbf{Z}_\mathbf{L}$ is the load impedance, and $\hat{\mathbf{V}}_\mathbf{0}$, $\hat{\mathbf{I}}_\mathbf{0}$ and $\hat{\mathbf{V}}_\mathbf{L}$, $\hat{\mathbf{I}}_\mathbf{L}$ are the voltage and current phasors at the two ends of the MTL.

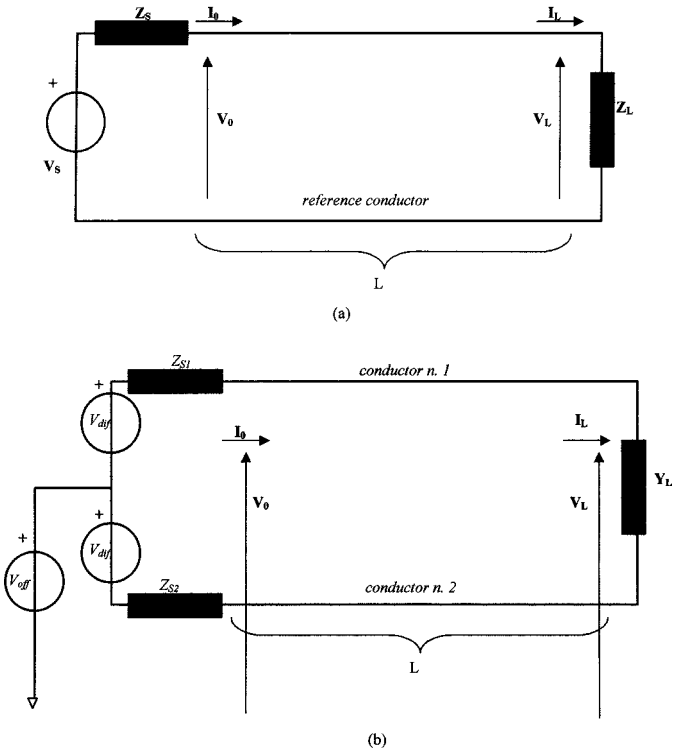

Fig. 2. Equivalent circuit for the MTL modeling. (a) Single-ended and (b) differential terminations.

A. The Parameter Extraction

The p.u.l. matrices for the impedance $\mathbf{Z}(\omega)$ and admittance $\mathbf{Y}(\omega)$ must first be evaluated to construct the MTL model. The $\mathbf{Z}(\omega)$ matrix takes into account the series effects of the resistance and inductance of the conductors. The evaluation of $\mathbf{Z}(\omega)$ is not discussed in this work, and the reader is referred to [10] for more details. The model adopted in this work allows the entries of the $\mathbf{Z}(\omega)$ matrix to be analytically evaluated at every frequency considered. The admittance matrix $\mathbf{Y}(\omega)$ given by

$$\mathbf{Y}(\omega) = \mathbf{G}(\omega) + j\omega\mathbf{C}(\omega) \tag{1}$$

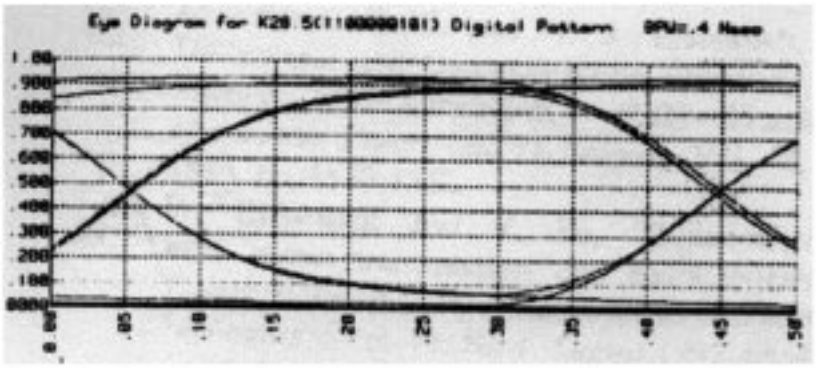

(a)

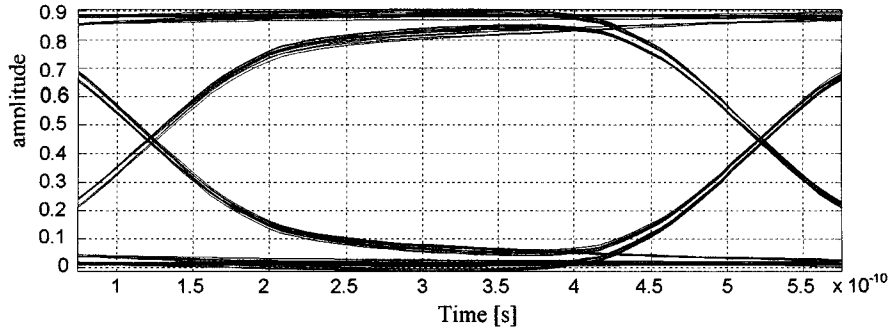

(b)

Fig. 3. (a) Eye patterns for a differential line: results from [7], vertical axis between 0.0 and 1.0 V, horizontal axis between 0.0 and 0.50 ns. (b) Eye patterns for a differential line: simulated data using the proposed TFTD approach.

is related to the frequency-dependent properties of the dielectric material. Starting from a knowledge of the dielectric permittivity $\varepsilon(\omega^*)$, and the dissipation factor $\tan\delta(\omega^*)$, measured at the discrete frequencies ω^*, the losses in the dielectric material are included in $\mathbf{Y}(\omega)$ by solving for the complex capacitance matrix $\hat{\mathbf{C}}(\omega^*)$ for a medium having complex permittivity $\hat{\varepsilon}(\omega^*)$

$$\hat{\varepsilon}(\omega^*) = \varepsilon(\omega^*)[1 - j\tan\delta(\omega^*)]. \tag{2}$$

Then, the standard procedure for calculating the p.u.l. capacitance matrix is modified by substituting $\varepsilon(\omega^*)$ with $\hat{\varepsilon}(\omega^*)$. Once $\hat{\mathbf{C}}(\omega^*)$ is evaluated, then $\mathbf{Y}(\omega)$ in (1) becomes

$$\begin{aligned}\mathbf{Y}(\omega^*) &= \mathbf{G}(\omega^*) + j\omega^*\mathbf{C}(\omega^*) \\ &= -\omega^* \operatorname{Im}\left(\hat{\mathbf{C}}(\omega^*)\right) + j\omega^* \operatorname{Re}\left(\hat{\mathbf{C}}(\omega^*)\right)\end{aligned} \tag{3}$$

with $\mathbf{G}(\omega^*) = -\omega^* \operatorname{Im}(\hat{\mathbf{C}}(\omega^*))$ and $\mathbf{C}(\omega^*) = \operatorname{Re}(\hat{\mathbf{C}}(\omega^*))$.

The elements of the p.u.l. matrices $\mathbf{Z}(\omega)$ and $\mathbf{Y}(\omega)$ are required at frequencies ω different from ω^* in the MTL equation solution process. For the evaluation of the admittance matrix, an interpolation among the values of $\varepsilon(\omega^*)$ and of $\tan\delta(\omega^*)$ is needed to compute the new values of $\hat{\varepsilon}(\omega)$ and $\hat{\mathbf{C}}(\omega)$, in order to obtain $\mathbf{Y}(\omega)$ from (3). This interpolation should be done taking into account the specific characteristics of the measurement techniques for $\varepsilon(\omega^*)$ and $\tan\delta(\omega^*)$. Standard techniques for measuring $\varepsilon(\omega)$ are relatively insensitive to measurement errors [13]. Consequently, the measured values do not have a significant variation about the correct value and show a linear trend. In this case, a linear interpolation of the samples is suitable to compute the new values of permittivity. By contrast, the measurement of the loss tangent is very sensitive to measurement errors [13], and the measured values are scattered about the actual trend. In this case, a simple linear interpolation of the samples would introduce an unrealistic behavior of the material. For this reason the values of $\tan\delta(\omega)$ are fitted using a least-square error-fitting procedure [14]. An interpolating two-exponential function as (4) was used at the beginning

$$f_1 = K_0 + ae^b + ce^d \tag{4}$$

but for all the material considered in this work a single exponential, with the parameters $K_0 = 8.16\ 10^{-4}$, $a = 1.83\ 10^{-2}$, and $b = 4.30\ 10^{-11}$, was found to be adequate.

B. The MTL Solution

The phasor voltages and currents at the two ends of the line are related with the chain parameter matrix $\hat{\mathbf{\Phi}}_{\mathbf{ij}}$ as

$$\hat{\mathbf{V}}_{\mathbf{L}} = \hat{\mathbf{\Phi}}_{11}(L)\hat{\mathbf{V}}_0 + \hat{\mathbf{\Phi}}_{12}(L)\hat{\mathbf{I}}_0 \tag{5}$$

$$\hat{\mathbf{I}}_{\mathbf{L}} = \hat{\mathbf{\Phi}}_{21}(L)\hat{\mathbf{V}}_0 + \hat{\mathbf{\Phi}}_{22}(L)\hat{\mathbf{I}}_0. \tag{6}$$

The expressions for the evaluation of the matrix entries $\hat{\mathbf{\Phi}}_{ij}$ in (5) and (6) are detailed in the Appendix. In the following the development, the notation $\hat{\mathbf{\Phi}}_{ij}(L) = \hat{\mathbf{\Phi}}_{ij}$ is used. Equations (5) and (6) along with the matrix equations for the terminations allow the voltages $\hat{\mathbf{V}}_{\mathbf{0}}$, $\hat{\mathbf{V}}_{\mathbf{L}}$ $\hat{\mathbf{I}}_{\mathbf{0}}$, and $\hat{\mathbf{I}}_{\mathbf{L}}$ and the currents $\hat{\mathbf{I}}_{\mathbf{0}}$ and $\hat{\mathbf{I}}_{\mathbf{L}}$ at the source and load ends to be evaluated as

$$\hat{\mathbf{V}}_0 = \hat{\mathbf{V}}_{\mathbf{S}} - \mathbf{Z}_{\mathbf{S}}\mathbf{A}^{-\mathbf{1}}\mathbf{B}\hat{\mathbf{V}}_{\mathbf{S}} \tag{7a}$$

$$\hat{\mathbf{V}}_{\mathbf{L}} = \mathbf{Z}_{\mathbf{L}}\hat{\mathbf{I}}_{\mathbf{L}} \tag{7b}$$

$$\hat{\mathbf{I}}_0 = \mathbf{A}^{-\mathbf{1}}\mathbf{B}\hat{\mathbf{V}}_{\mathbf{S}} \tag{7c}$$

$$\hat{\mathbf{I}}_{\mathbf{L}} = \mathbf{\Phi}_{21}\hat{\mathbf{V}}_{\mathbf{S}} - \hat{\mathbf{\Phi}}_{21}\mathbf{Z}_{\mathbf{S}}\mathbf{A}^{-\mathbf{1}}\mathbf{B}\hat{\mathbf{V}}_{\mathbf{S}} + \hat{\mathbf{\Phi}}_{22}\mathbf{A}^{-\mathbf{1}}\mathbf{B}\hat{\mathbf{V}}_{\mathbf{S}} \tag{7d}$$

where

$$\mathbf{A} = -\mathbf{Z_L}\hat{\mathbf{\Phi}}_{21}\mathbf{Z_S} + \mathbf{Z_L}\hat{\mathbf{\Phi}}_{22} + \hat{\mathbf{\Phi}}_{11}\mathbf{Z_S} - \hat{\mathbf{\Phi}}_{12} \quad (8a)$$

$$\mathbf{B} = \hat{\mathbf{\Phi}}_{11} - \mathbf{Z_L}\hat{\mathbf{\Phi}}_{21}. \quad (8b)$$

Equations (7a)–(7d) are then solved at each frequency ω, contained in the frequency spectrum of the PRBS, and the harmonic components of the termination voltages are obtained. Finally, the corresponding waveforms in time domain are computed using an IFFT, and the eye pattern is generated.

The line configuration for differential terminations is shown in Fig. 2(b). The matrix equation for a differential source is

$$\hat{\mathbf{V}}_0 = \hat{\mathbf{V}}_\mathbf{S} - \mathbf{Z_S}\hat{\mathbf{I}}_0 \quad (9a)$$

and for the differential load

$$\hat{\mathbf{I}}_\mathbf{L} = \mathbf{Y_L}\hat{\mathbf{V}}_\mathbf{L} \quad (9b)$$

where

$$\hat{\mathbf{V}}_\mathbf{S} = \begin{bmatrix} V_{\text{off}} + V_{\text{dif}} \\ V_{\text{off}} - V_{\text{dif}} \end{bmatrix} \quad (10a)$$

$$\mathbf{Z_S} = \begin{bmatrix} Z_{S1} & 0 \\ 0 & Z_{S2} \end{bmatrix} \quad (10b)$$

$$\mathbf{Y_L} = \begin{bmatrix} 1/Z_L & -1/Z_L \\ -1/Z_L & 1/Z_L \end{bmatrix} \quad (10c)$$

and V_{dif} is the differential source voltage, and V_{off} is an offset. By substituting (9) into (5), the source and load voltages and currents are then

$$\hat{\mathbf{V}}_0 = \hat{\mathbf{V}}_\mathbf{S} - \mathbf{Z_S}\mathbf{A^{-1}}\mathbf{B}\hat{\mathbf{V}}_\mathbf{S} \quad (11a)$$

$$\hat{\mathbf{I}}_0 = \mathbf{A^{-1}}\mathbf{B}\hat{\mathbf{V}}_\mathbf{S} \quad (11b)$$

$$\hat{\mathbf{V}}_\mathbf{L} = \hat{\mathbf{\Phi}}_{11}\hat{\mathbf{V}}_\mathbf{S} - \hat{\mathbf{\Phi}}_{11}\mathbf{Z_S}\mathbf{A^{-1}}\mathbf{B}\hat{\mathbf{V}}_\mathbf{S} + \hat{\mathbf{\Phi}}_{12}\mathbf{A^{-1}}\mathbf{B}\hat{\mathbf{V}}_\mathbf{S} \quad (11c)$$

$$\hat{\mathbf{I}}_\mathbf{L} = \mathbf{Y_L}\hat{\mathbf{V}}_\mathbf{L} \quad (11d)$$

where

$$\mathbf{A} = \mathbf{Y_L}\hat{\mathbf{\Phi}}_{11}\mathbf{Z_S} + \mathbf{Y_L}\hat{\mathbf{\Phi}}_{12} - \hat{\mathbf{\Phi}}_{21}\mathbf{Z_S} + \hat{\mathbf{\Phi}}_{22} \quad (12a)$$

$$\mathbf{B} = \mathbf{Y_L}\hat{\mathbf{\Phi}}_{11} - \hat{\mathbf{\Phi}}_{21}. \quad (12b)$$

The source and load voltage and current solutions for the single-ended and differential terminated cases are then complete.

III. Eye Pattern Measurements and Simulations

The validation of the proposed procedure was carried out by comparing the results with those obtained from other techniques and from measurement. First, eye pattern results from [7] are compared with those simulated using the MTL approach considered in this work. Fig. 3(a) shows the eye pattern for a differential line on an FR4 board (Nelco N4000-6, fiber glass/epoxy resin). The data rate was 2.5 Gb/s. This eye pattern was generated from the measurement of the mixed mode S-parameter data on a differential line by convolving the time-domain impulse response of S_{DD21} with the standard K28.5 bit pattern (1 100 000 101). Fig. 3(b) shows the eye pattern computed by means of the TFTD approach. The appropriate metrics of the eye pattern are: 1) its maximum eye opening (MEO), defined as the maximum difference, at the same time instant, between points in the interior of the eye patter; and 2) its maximum eye width (MEW), defined as the maximum difference, at the same voltage level, between two points in the interior of the eye pattern. These two points correspond to the decision threshold, i.e., the region of the eye pattern in which the bits' fronts intersect. A comparison between the results from [7] and the results calculated using the MTL approach is summarized in Table I.

TABLE I
Comparison Between Eye Patterns in Fig. 3(a) and (b)

	Eye Pattern Fig. 3a (from [7])	Eye Pattern Fig. 3b
Maximum Eye Opening (mV)	760	770
Maximum Eye Width (ps)	392	394

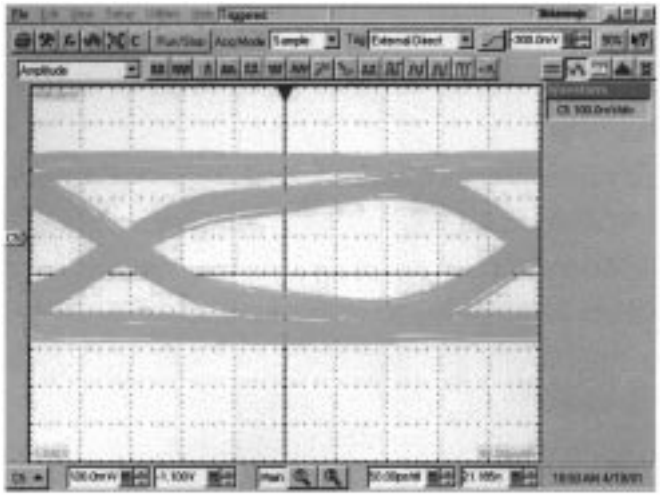

(a)

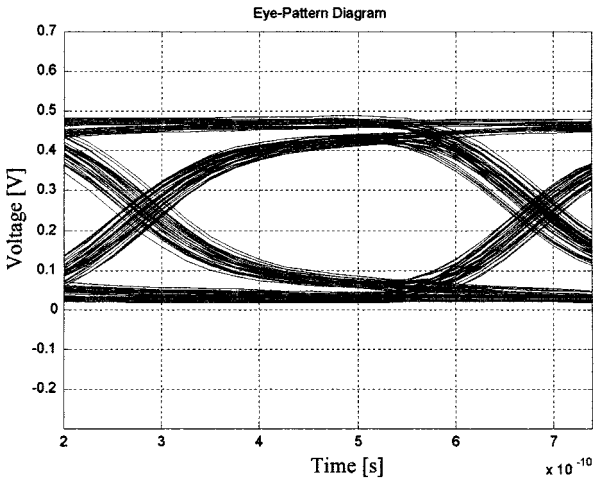

(b)

Fig. 4. The eye pattern (a) measured and (b) computed using the TFTD approach.

A second comparison was performed between the MTL approach and measurements. In a single-ended 50 -Ω stripline, an HP 70841B pattern generator was used to launch a $2^7 - 1$ PRBS, nonreturn to zero (NRZ), coded at 2.5 Gb/s. The board dielectric material had frequency-dependent values of ε_r and loss tangent similar to those of the class of Rogers-like resins. The trace was terminated in the 50 —Ω input impedance of the Tektronix Communication Signal Analyzer CSA 8000, used to display the eye pattern at the load. The measured results are shown in Fig. 4(a). The trace was then terminated in a matched load.

TABLE II
COMPARISON BETWEEN EYE PATTERNS IN FIG. 4(a) AND (b)

	Eye Pattern Fig. 4a (measurement)	Eye Pattern Fig. 4b
Maximum Eye Opening (mV)	280	285
Maximum Eye Width (ps)	330	325

The eye pattern calculated with the MTL approach is shown in Fig. 4(b), and a summary of the comparison of the MEO and MEW for this configuration is given in Table II.

The procedure was further validated using a ten-layer test board that was a mix of glass fiber and epoxy resin (an FR4-like material) denoted Board $\mathbf{A}$ and an eight-layer test board in glass reinforced hydrocarbon/ceramic laminates and pre-preg with low dielectric losses, denoted Board $\mathbf{B}$. These boards have been specifically designed for these tests and are not made to accommodate active signal drivers, because of this there is no need of power planes but only ground (GND) planes. The PCBs were 50 cm in length and 40 cm in width. The layer stack-up is given, together with the layer and plane thicknesses for Board $\mathbf{A}$ and Board $\mathbf{B}$, in the photographs in Fig. 5(a) and (b), respectively. The photographs were generated with an optical microscope. On each board, 50-Ω single-ended and 100-Ω differential edge-coupled microstrip and stripline traces, with lengths of 50 cm were laid out. To compare the eye-pattern measurement with the MTL simulations, only 50-Ω single-ended microstrip and striplines were considered. The trace dimensions of the two cases were different in order to control the value of the nominal characteristic impedance. For Board $\mathbf{A}$, the trace widths were $w_{\mathbf{A}\mu} = 250$ μm for the microstrip (Layer 1), and $w_{\mathbf{A}s} = 200$ μm for the stripline (Layer 3), and for Board $\mathbf{B}$, $w_{\mathbf{B}\mu} = 330$ μm (Layer 1), and $w_{\mathbf{B}s} = 210$ μm (Layer 3). Half-ounce copper was used for the metallization thickness. These values are in the range of those commonly used in present high-speed digital systems technology. The above mentioned pattern generator was connected to the boards through SMA connectors, and the traces were driven with a $2^7 - 1$ PRBS, NRZ, coded at 2.5 Gb/s. The bit sequence swing was 500 mV and the nominal rise/fall time of the bit pulse was 120 ps, as shown by the eye pattern of the input bit sequence in Fig. 6, measured at the output of the generator. As shown in Fig. 6, the presence of jitter inherent to the input sequence is apparent. This jitter was subtracted from that measured at the end of the line, in order to correctly estimate the effects of the frequency-dependent properties of the board material on the integrity of the digital signal.

The frequency-dependent properties of the Board $\mathbf{A}$ material are shown in Fig. 2. The dielectric laminate of Board $\mathbf{B}$ exhibits an almost constant dielectric constant and loss tangent over a broad frequency range as shown in Fig. 7. The reference values at 10 GHz are for the laminate $\varepsilon_{r\_\text{laminate}} = 3.3$, $\tan\delta = 0.002$, and for the pre-preg $\varepsilon_{r\_\text{pre-preg}} = 3.17$, assuming for the latter the same loss tangent as the laminate [15].

Figs. 8 and 9 show the measured eye pattern at the end of the microstrips and striplines on Board $\mathbf{A}$ and Board $\mathbf{B}$. The difference between the eye pattern at the ends of the microstrip and stripline traces on the same board is negligible. In these cases, the maximum-eye-opening and maximum-eye-width values of the four traces almost coincide. The role of the ISI in displacing

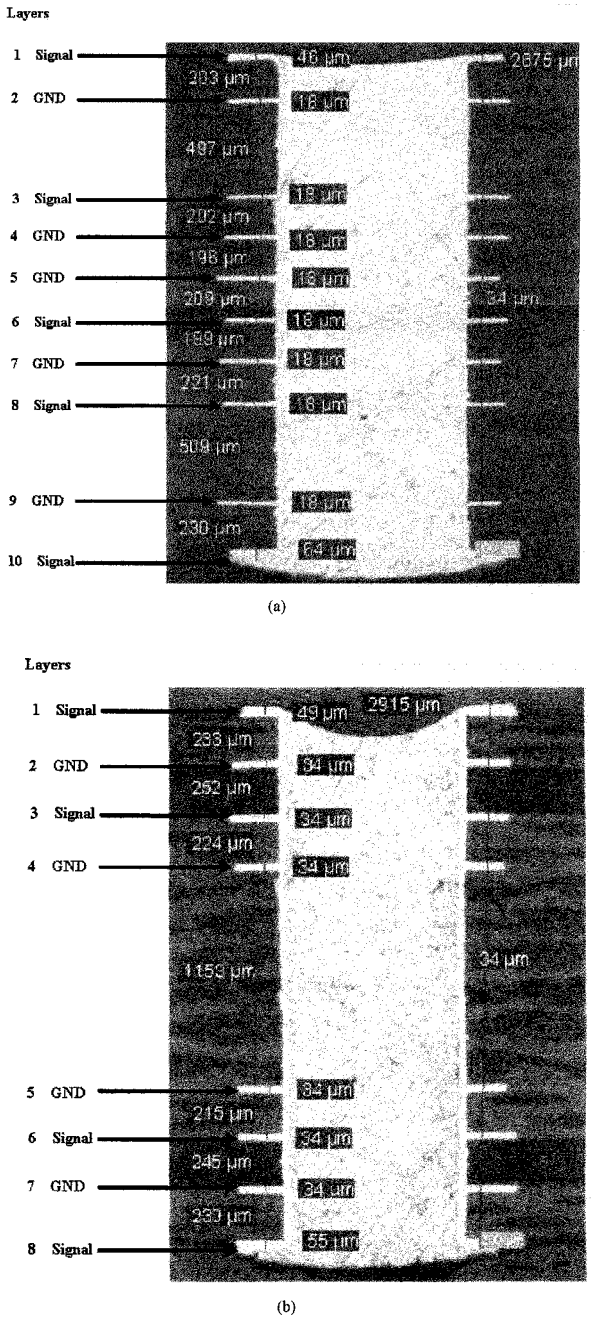

Fig. 5. An optical microscopic photograph of the layer stack-up cross section. (a) Board $\mathbf{A}$. (b) Board $\mathbf{B}$.

the actual data transition times from the ideal, i.e., the time jitter of the data signals at the end of the traces, is also illustrated in the eye patterns shown in Figs. 8 and 9. The time jitter can be evaluated as

$$J = 0.5(T_{ui} - \text{MEW}) \tag{13}$$

where T_{ui} is the time interval defined as $T_{ui} = 1/\text{bitrate}$. For this study, $T_{ui} = 400$ ps for 2.5 Gb/s. One measure of the eye pattern opening (or closing) is the percentage difference Δ_{MEO} between the MEO values of Board $\mathbf{A}$ and Board $\mathbf{B}$, defined as

$$\Delta_{\text{MEO}}\ \% = |\text{MEO}_{\mathbf{A}} - \text{MEO}_{\mathbf{B}}|/\text{MEO}_{\mathbf{B}}\ \%. \tag{14}$$

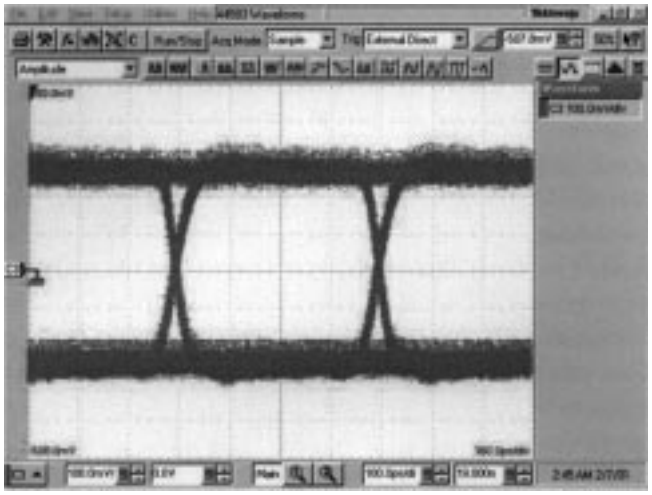

Fig. 6. The eye pattern of the input PRBS, $2^7 - 1$, NRZ coded, with a rise time = 120 ps, and data rate = 2.5 Gb/s. (Scale: 100 ps/div, 60 mV/div.)

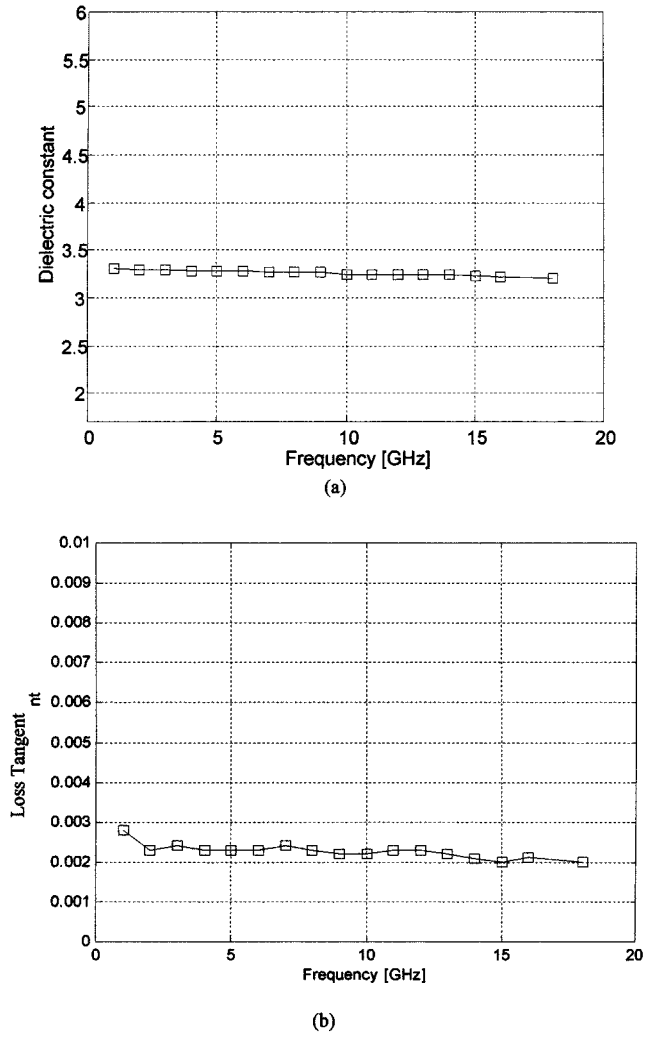

Fig. 7. Measured and linearly interpolated values $\tan\delta(\omega)$ for the glass-reinforced, hydrocarbon/ceramic laminates material. (a) $\varepsilon_r(\omega)$. (b) $\tan\delta(\omega)$.

Considering the eye patterns in Figs. 8(b) and 9(b), the measured values are for Board $\mathbf{A}$ $\mathrm{MEO}_{\mathbf{A}} = 240$ mV, for Board $\mathbf{B}$

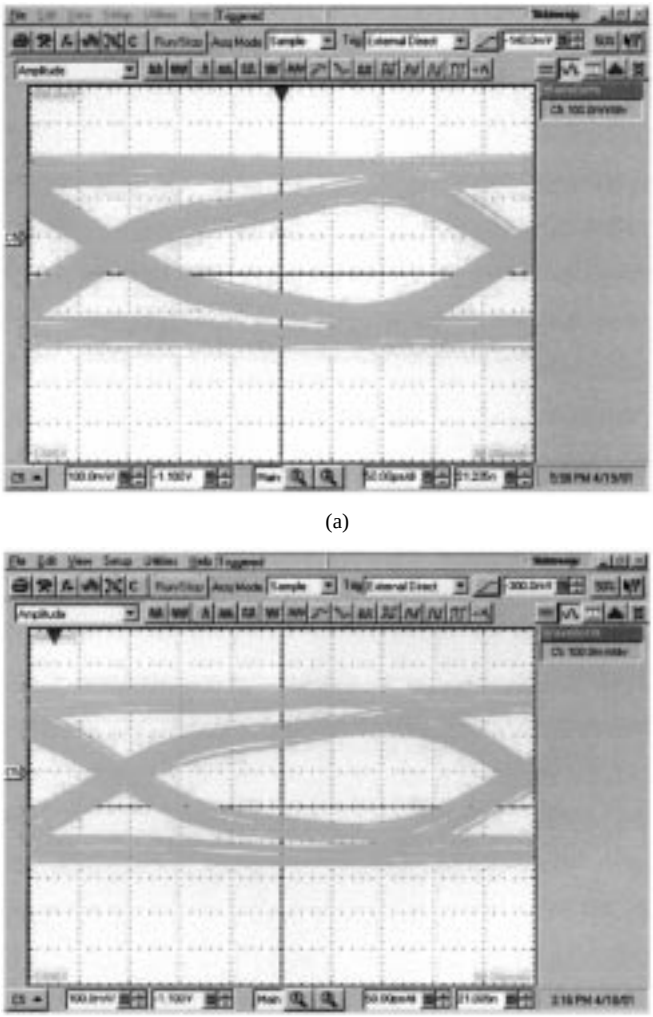

(a)

(b)

Fig. 8. Measured eye pattern at the end of the transmission line. (a) Microstrip line on Layer 1 of Board $\mathbf{A}$. (b) Stripline on Layer 3 of Board $\mathbf{A}$.

$\mathrm{MEO}_{\mathbf{B}} = 280$ mV, and from (14) $\Delta_{\mathrm{MEO}} = 14.2\%$. This last value is in the range of that obtained by considering the eye pattern height values reported in [7, Table 2] for similar materials such as N4000-6 and Metclad. From these values, one obtains $\Delta_{\mathrm{MEO}} = 11.6\%$.

From these considerations, one can infer that for the specific configuration of a digital signal at 2.5 Gb/s transmitted on a PCB trace 50-cm long, the dielectric losses of the material are not a concern for the SI if a 14% closing of the eye pattern is acceptable by the designer. Consequently, for data rates slower than 2.5 Gb/s, and traces shorter than 50 cm, it may be sufficient to use an ordinary low-cost FR4 dielectric material to lay out traces with controlled impedance on a board, without resorting to more expensive, low-loss dielectric materials. The proposed MTL modeling approach allows the SI attributes of the structures to be assessed for different board materials and traces' length. The computed values of MEO for two striplines with cross sections and dielectric materials identical to those of Board $\mathbf{A}$ and Board $\mathbf{B}$ are shown in Fig. 10. In this case, though, the line lengths were varied from 25 to 90 cm. The computed values of MEW for the same structures and boards are shown in Fig. 11. From Fig. 10, one can predict that, for the configurations

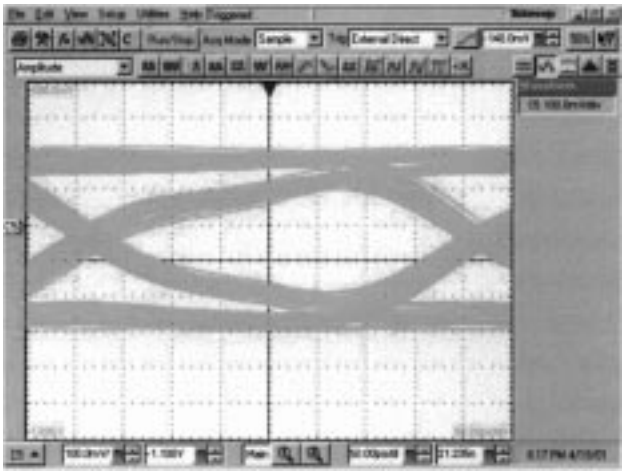

(a)

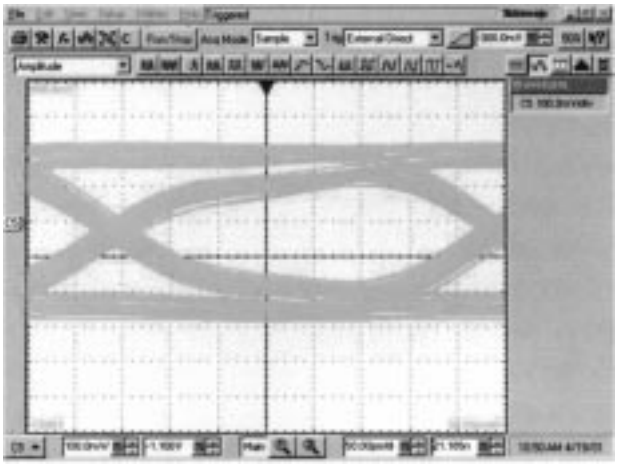

(b)

Fig. 9. Measured eye pattern at the end of the transmission line. (a) Microstrip line on Layer 1 of Board $\mathbf{B}$. (b) Stripline on Layer 3 of Board $\mathbf{B}$.

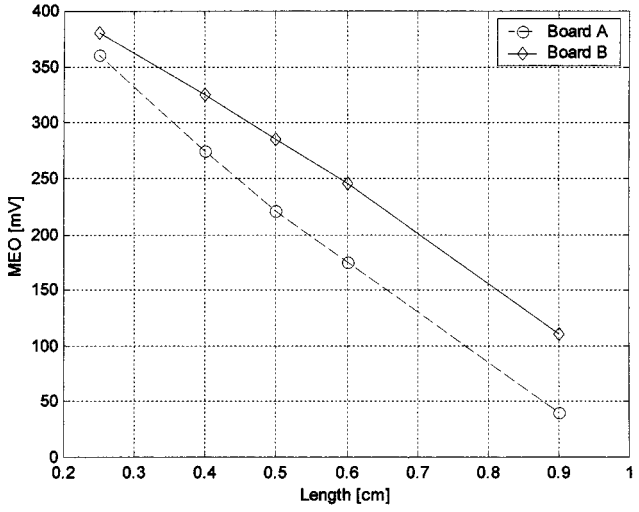

Fig. 10. Predicted MEO for different lengths of the stripline at 2.5 Gb/s.

considered, the eye opening (measured by the MEO values) degrades for traces length greater than 55–60 cm in FR4-like materials. The same trend is found in Fig. 11 for the temporal width

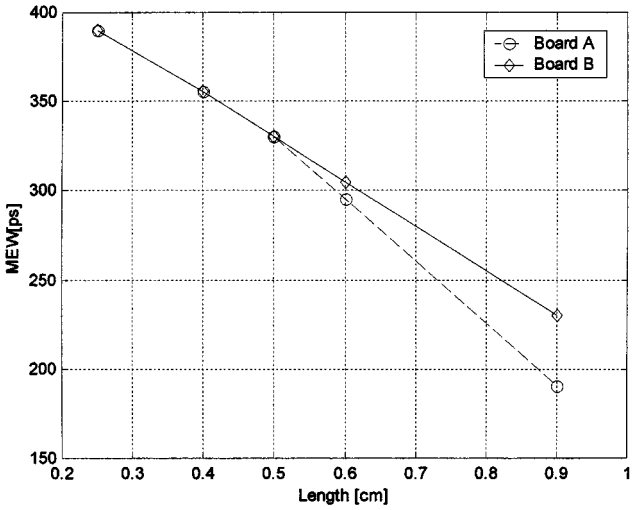

Fig. 11. Predicted MEW for different lengths of the stripline at 2.5 Gb/s.

of the bit pattern although the magnitude of the MEW values is not a concern in this case. As expected by its values of $\varepsilon_r(\omega)$ and $\tan\delta(\omega)$, the glass reinforced hydrocarbon/ceramic material exhibits a better performance at the present bit rate in all the considered range of lengths. From Fig. 10, degradation is less significant for the signals traveling on large backplanes of Board $\mathbf{B}$ material than Board $\mathbf{A}$ material.

IV. Conclusion

A modeling approach for evaluating the impact of the frequency-dependent properties of dielectric laminates on SI in high-speed PCBs at the design stage can be very beneficial. The time and expense of many measurements can be minimized. In this work, an approach based on MTL modeling that requires only a knowledge of the dielectric constant and dissipation factor versus frequency has been presented. The approach compares well with other published results and measurements. The measurements, carried out on specially designed test boards, showed that digital signals at data rates lower than 2.5 Gb/s, transmitted on traces with controlled impedances and lengths shorter than 50 cm, do not require PCB materials with low dielectric losses. For the considered configurations and materials, currently used in the telecommunications and computer industries, a variation of eye pattern opening of around 14% has been measured and computed between a standard, low-cost FR4 material and a low-loss material. Although the issue of whether an eye opening degradation is a concern or not rests on the bit error rate (BER) design requirement for the link in question, the quantitative knowledge of such a degradation is beneficial for a BER estimation. The MTL approach detailed herein can be used for further investigations on the SI impact of the frequency-dependent losses of conductors and dielectric materials for bit rates higher than 2.5 Gb/s. The proposed method allows for the evaluation of the MEO and MEW for various "what-if" scenarios to detail behavioral trends of the effects on the digital signals.

APPENDIX

The expressions for evaluating the chain parameter matrices $\hat{\mathbf{\Phi}}_{\mathbf{ij}}(L)$ are given by [10]

$$\hat{\mathbf{\Phi}}_{\mathbf{11}}(L) = \frac{1}{2}\mathbf{Y}^{-1}\mathbf{T}\left(\mathbf{e}^{\gamma L} + \mathbf{e}^{-\gamma L}\right)\mathbf{T}^{-1}\mathbf{Y} \quad \text{(A1a)}$$

$$\hat{\mathbf{\Phi}}_{\mathbf{12}}(L) = -\frac{1}{2}\mathbf{Z}_C\left[\mathbf{T}\left(\mathbf{e}^{\gamma L} - \mathbf{e}^{-\gamma L}\right)\mathbf{T}^{-1}\right] \quad \text{(A1b)}$$

$$\hat{\mathbf{\Phi}}_{\mathbf{21}}(L) = -\frac{1}{2}\left[\mathbf{T}\left(\mathbf{e}^{\gamma L} - \mathbf{e}^{-\gamma L}\right)\mathbf{T}^{-1}\right]\mathbf{Y}_C \quad \text{(A1c)}$$

$$\hat{\mathbf{\Phi}}_{\mathbf{22}}(L) = \frac{1}{2}\mathbf{T}\left(\mathbf{e}^{\gamma L} + \mathbf{e}^{-\gamma L}\right)\mathbf{T}^{-1} \quad \text{(A1d)}$$

where $\mathbf{T}$ is the modal transformation matrix defined by

$$\mathbf{T}^{-1}\mathbf{YZT} = \gamma^2. \quad \text{(A2)}$$

The matrix γ is the diagonal matrix of the modal propagation constants γ, and $\mathbf{Z}_C$ and $\mathbf{Y}_C$ are the characteristic impedance and admittance matrices, respectively, given by

$$\mathbf{Z}_C = \mathbf{Z}\left(\sqrt{\mathbf{YZ}}\right)^{-1} \quad \text{(A3a)}$$

$$\mathbf{Y}_C = \mathbf{Z}_C^{-1}. \quad \text{(A3b)}$$

ACKNOWLEDGMENT

The authors thank Dr. J. Knighten and Dr. J. Fan of NCR for providing the needed information for one of the performed tests and helpful discussions.

REFERENCES

[1] *International Technology Roadmap for Semiconductors, 1999 Edition*. San Jose, CA: Semiconduct. Indus. Assoc., Mar. 2000.
[2] B. Ahmad and J. Cain, "Performance evaluation of high speed serial links," in *Proc. Design Conf.*, Santa Clara, CA, Jan. 29–Feb. 1, 2001.
[3] D. Miller, "Modeling loss and jitter in high-speed serial connects," in *Proc. DesignCon2001*, Santa Clara, CA, Jan. 29–Feb. 1, 2001.
[4] V. Ricchiuti, "Propagation of high-speed digital signals on printed circuit boards," *Future Circuits Int.*, no. 5, pp. 45–50, June 1999.
[5] P. Galloway, K. Roselle, and R. Cutler, "Using creative silicon technology to extend the useful life of backplane and card substrates at 3.125 Gbps and beyond," in *Proc. Design Conf.*, Santa Clara, CA, Jan. 29–Feb. 1, 2001.
[6] C. Morgan and D. Helster, "New printed-wiring-board materials guard against garbled gigabits," *EDN*, vol. 11, pp. 134–141, November 1999.
[7] V. Adamian, J. Knighten, N. Smith, B. Cole, P. Phillips, R. Alexander, and J. Fan, "Characterization of printed circuit board transmission lines at data rate above 1Gb/s using time domain characteristics derived from frequency domain measurements," in *Proc. 14th Int. Zurich Electromagn. Compat. Symp.*, Zurich, Switzerland, Feb. 20–22, 2001.
[8] T. Hochberg, H. Merkelo, and M. Resso, "Advances in high-speed design in dispersively attenuating environments such as cables and backplanes," in *Proc. DesignCon2001*, Santa Clara, CA, Jan. 29–Feb. 1, 2001.
[9] T. Hochberg, H. Merkelo, G. Kimitsuka, J. Grebenkemper, and D. Vermeersch, "Broadband measurements in the differential mode: Accurate determination of dispersive attenuation," in *Proc. Design Conf.*, Santa Clara, CA, Jan. 29–Feb. 1, 2001.
[10] C. R. Paul, *Analysis of Multiconductor Transmission Line*. New York: Wiley, 1996.
[11] A. Taflove, *Computational Electrodynamics—The Finite-Difference Time-Domain Method*. Norwood, MA: Artech House, 1995.
[12] H. A. Wheeler, "Formulas for skin effect," *Proc. IRE*, vol. 30, pp. 412–424, 1942.
[13] R. H. Voelker, G.-T. Lei, G.-W. Pan, and B. K. Gilbert, "Determination of complex permittivity of low-loss dielectrics," *IEEE Trans. Microwave Theory Tech.*, vol. 45, pp. 1955–1960, Oct. 1997.
[14] F. B. Hildebrand, *Introduction to Numerical Analysis*, 2nd ed. New York: Dover, 1974.
[15] D. I. Amey and S. J. Horowitz, "Material performance at frequencies up to 20 GHz," in *Proc. IEMT/IMC Conf.*, Omiya, Japan, Apr. 16–18, 1997.

Giulio Antonini (M'94) was born in Avezzano, Italy, on January 5, 1969. He received the Laurea degree *(summa cum laude)* in electrical engineering from the University of L'Aquila, L'Aquila, Italy, in 1994, and the Ph.D. degree in electrical engineering from the University of Rome "La Sapienza," Rome, Italy, in 1998.

Since 1998, he has been with the Department of Electrical Engineering of the University of L'Aquila. His research activities focus on EMC analysis and modeling of complex structures, lightning, shielding problems, emissions from power drive systems, and SI. Part of his research interests is in the field of fast numerical methods for the analysis of EMC problems. During the summers of 1998–2000, he was with the T. J. Watson Research Center (IBM) working on PEEC modeling.

Dr. Antonini is a member of the IEEE Electromagnetic Compatibility (EMC) Society TC-9 Committee. He was the recipient of the 1998 IEEE EMC Best Paper Award.

James L. Drewniak (S'85–M'90–SM'01) received the B.S., M.S., and Ph.D. degrees in electrical engineering from the University of Illinois at Urbana-Champaign, in 1985, 1987, and 1991, respectively.

He joined the Electrical Engineering Department, University of Missouri-Rolla, in 1991, where he is part of the Electromagnetic Compatibility Laboratory. His research includes electromagnetic compatibility in high-speed digital and mixed signal designs, electronic packaging, and electromagnetic compatibility in power-electronic-based systems.

Dr. Drewniak is an associate editor of the IEEE TRANSACTIONS ON ELECTROMAGNETIC COMPATIBILITY.

Antonio Orlandi (M'90–SM'97) was born in Milan, Italy, in 1963. He received the Laurea degree in electrical engineering from the University of Rome "La Sapienza," Italy, in 1988.

From 1988 to 1990, he was with the Department of Electrical Engineering, University of Rome "La Sapienza." He is currently a Full Professor with the Department of Electrical Engineering, University of L'Aquila, L'Aquila, Italy. He has authored and coauthored papers in the field of electromagnetic compatibility in lightning protection systems and power drive systems. His current research interests are in the field of numerical methods and modeling techniques to approach SI issues in high-speed digital systems.

Dr. Orlandi is member of the Education, TC-9 Computational Electromagnetics and TC-10 Signal Integrity Committees of the IEEE Electromagnetic Compatibility (EMC) Society, and chairman of the "EMC INNOVATION" Technical Committee of the International Zurich Symposium and Technical Exhibition on EMC. He was the recipient of the 1997 IEEE TRANSACTIONS ON ELECTROMAGNETIC COMPATIBILITY Best Paper Award.

Vittorio Ricchiuti (M'99–SM'02) received the Laurea degree in electronic engineering from the University of Pisa, Pisa, Italy, in 1989.

In 1989, he joined Italtel Transmission Laboratories in L'Aquila, L'Aquila, Italy, where he has been working in the field of data transmission via low-voltage and middle-voltage electrical power network for load management. Since November 1993, his interest is in the field of high-speed data transmission networks (SDH hierarchy). Since November 1999, he has been with Siemens Information and Communication Networks, L'Aquila, Italy. In the last three years, he has worked on high-speed PCB design as an SI Engineer. His main research interests include power bus decoupling on complex high-speed PCBs for telecommunication equipments and low losses dielectric materials for PCB manufacturing.